

4

DTIC FILE COPY

AD-A206 547

OFFICE OF NAVAL RESEARCH

GRANT N00014-89-J-1178

R&T Code 413q001-01

TECHNICAL REPORT NO. 25

Effects of Thermal History on Stress-Related Properties of Very Thin Films of Thermally Grown Silicon Dioxide, SiO₂

by

J.T. Fitch^a, E. Kobeda^b, G. Lucovsky^a and E.A. Irene^b

Prepared for Publication

in the

The Journal of Vacuum Science and Technology

^aNorth Carolina State University
Department of Physics and Materials Science and Engineering
Raleigh, NC

^bUniversity of North Carolina
Department of Chemistry
Chapel Hill, NC

DTIC
ELECTRONIC
MAR 30 1989
S H D

Reproduction in whole or in part is permitted for any purpose of the United States Government.

This document has been approved for public release and sale; its distribution is unlimited.

89 3 30 091

REPORT DOCUMENTATION PAGE

1a. REPORT SECURITY CLASSIFICATION Unclassified		1b. RESTRICTIVE MARKINGS	
2a. SECURITY CLASSIFICATION AUTHORITY		3. DISTRIBUTION/AVAILABILITY OF REPORT Approved for public release; distribution unlimited.	
2b. DECLASSIFICATION/DOWNGRADING SCHEDULE			
4. PERFORMING ORGANIZATION REPORT NUMBER(S) Technical Report #25		5. MONITORING ORGANIZATION REPORT NUMBER(S)	
6a. NAME OF PERFORMING ORGANIZATION UNC Chemistry Dept.	6b. OFFICE SYMBOL (If applicable)	7a. NAME OF MONITORING ORGANIZATION Office of Naval Research (Code 413)	
6c. ADDRESS (City, State and ZIP Code) CB# 3290, Venable Hall University of North Carolina Chapel Hill, NC 27599-3290		7b. ADDRESS (City, State and ZIP Code) Chemistry Program 800 N. Quincy Street Arlington, Virginia 22217	
8a. NAME OF FUNDING/SPONSORING ORGANIZATION Office of Naval Research	8b. OFFICE SYMBOL (If applicable)	9. PROCUREMENT INSTRUMENT IDENTIFICATION NUMBER Grant #N00014-89-J-1178	
8c. ADDRESS (City, State and ZIP Code) Chemistry Program 800 N. Quincy Street, Arlington, VA 22217		10. SOURCE OF FUNDING NOS.	
		PROGRAM ELEMENT NO.	PROJECT NO.
		TASK NO.	WORK UNIT NO.
11. TITLE (Include Security Classification) EFFECTS OF THERMAL HISTORY ON STRESS-RELATED PROPERTIES OF VERY THIN FILMS OF THERMALLY GROWN SILICON DIOXIDE			
12. PERSONAL AUTHOR(S) E.A. Irene			SiO ₂
13a. TYPE OF REPORT Interim Technical	13b. TIME COVERED FROM _____ TO _____	14. DATE OF REPORT (Yr., Mo., Day) March 14, 1989	15. PAGE COUNT 37
16. SUPPLEMENTARY NOTATION			
17. COSATI CODES		18. SUBJECT TERMS (Continue on reverse if necessary and identify by block number)	
FIELD	GROUP	SUB. GR.	
19. ABSTRACT (Continue on reverse if necessary and identify by block number) <i>AV6STR0M5</i> This paper presents studies of the infrared (ir) absorbance and the intrinsic stress in thermally grown very thin films (60Å to 700Å) of silicon dioxide, SiO ₂ . These data are combined with previously obtained data for thicker thermally grown films (approximately 1200Å) to study the variation in intrinsic growth stress close to the Si/SiO ₂ interface. The combined data indicate that the intrinsic stress at Si/SiO ₂ interfaces extrapolates to the same relatively high values for oxides grown at 700°C and 1000°C, and that the distribution of Si-O-Si bond angles close to the Si/SiO ₂ interface, as deduced from the ir data, is quantitatively different than in the bulk of the oxide film. These two observations are explained in terms of a model based on a temperature dependent viscoelastic relaxation of the oxide stress. This model emphasizes differences in the thermal history of the SiO ₂ near the Si/SiO ₂ interface, as compared to the SiO ₂ that is well-removed from that interface and is in the bulk of the film and/or close to the 'top' surface of the film. (JE)			
20. DISTRIBUTION/AVAILABILITY OF ABSTRACT UNCLASSIFIED/UNLIMITED <input checked="" type="checkbox"/> SAME AS RPT. <input type="checkbox"/> DTIC USERS <input type="checkbox"/>		21. ABSTRACT SECURITY CLASSIFICATION Unclassified	
22a. NAME OF RESPONSIBLE INDIVIDUAL Dr. David L. Nelson		22b. TELEPHONE NUMBER (Include Area Code) (202) 696-4410	22c. OFFICE SYMBOL

Effects of Thermal History on Stress-Related Properties of Very Thin Films of Thermally Grown Silicon Dioxide, SiO₂

J.T. Fitch^a, E. Kobeda^b, G. Lucovsky^a and E.A. Irene^b

^aDepartments of Physics and Materials Science and Engineering, North Carolina State University, Raleigh, NC 27695-8202

^bDepartment of Chemistry, University of North Carolina, Chapel Hill, NC 27514

ABSTRACT

This paper presents studies of the infrared (ir) absorbance and the intrinsic stress in thermally grown very thin films (60Å to 700Å) of silicon dioxide, SiO₂. These data are combined with previously obtained data for thicker thermally grown films (approximately 1300Å) to study the variation in intrinsic growth stress close to the Si/SiO₂ interface. The combined data indicate that the intrinsic stress at Si/SiO₂ interfaces extrapolates to the same relatively high values for oxides grown at 700°C and 1000°C, and that the distribution of Si-O-Si bond angles close to the Si/SiO₂ interface, as deduced from the ir data, is quantitatively different than in the bulk of the oxide film. These two observations are explained in terms of a model based on a temperature dependent viscoelastic relaxation of the oxide stress. This model emphasizes differences in the thermal history of the SiO₂ near the Si/SiO₂ interface, as compared to the SiO₂ that is well-removed from that interface and is in the bulk of the film and/or close to the 'top' surface of the film. The observed differences between the 700°C and 1000°C bulk oxides, and the associated Si/SiO₂ interfaces are explained in terms of a renormalized time scale that is defined by the ratio of the growth time to the viscoelastic relaxation time at the growth temperature.



Accession For	
NTIS GRA&I	<input checked="" type="checkbox"/>
DTIC TAB	<input type="checkbox"/>
Unannounced	<input type="checkbox"/>
Justification	
By	
Distribution/	
Availability Codes	
Dist	Avail and/or Special
A-1	

differ by more than three orders of magnitude [6], whereas the times for oxide growth of films of equivalent thicknesses in a dry ambient at the same two temperatures only differ by about two to three orders of magnitude [7]. These relative differences in the two time scales are then shown in this paper to promote significant differences in the relative stress relief for the two growth temperatures we have examined. We explore effects of this non-uniform thermal history through: (1) comparisons of v and Δv as determined from the analysis of ir data in both the very thin and the thicker oxide films; (2) analysis of stress and ir data in terms of a Maxwell model [6,8] for viscoelastic relaxation of intrinsic growth stress; and (3) analysis of elastic properties of thin oxides films using a combination of stress and ir data.

II EXPERIMENTAL PROCEDURES

A. Sample Preparation

The substrate material used for oxide growth was of two types: 2 inch diameter, 75 μm thick, 2 $\Omega\text{-cm}$ p-type silicon wafers, and 4 inch diameter, 500 μm thick, 16-20 $\Omega\text{-cm}$ p-type silicon wafers. The 75 μm thick wafers were used for the stress measurements, and were scribed and broken into small strips, approximately 1 cm by 4 cm. The 4 inch diameter wafers were kept in tact and subjected to an HF/HNO₃ based etch (CP4A) to smooth the backside of the wafers and thereby reduce transmission losses in the ir measurements that would have been present due to the surface roughness of the as received wafers. Both sets of wafers were then processed in the same way prior to the thermal oxidation cycles at 700 and 1000°C [4]. The wafers were first subjected to a modified RCA clean, and then were preoxidized to grow approximately 1000Å of oxide. The oxide formed in this way was stripped in buffered HF. This preliminary oxidation step was used to remove contaminants from the Si surface prior to the final thermal oxidations. The silicon samples were then given a second modified RCA clean, and were oxidized in a double-walled, resistively-heated fused silica tube furnace at temperatures of 700°C and 1000°C. Silicon wafers were oxidized for different times to produce films with thicknesses between 60Å and 700Å. For the 700°C oxides this corresponds to oxidation times between about

20 hours and 500 hours, and for the 1000°C oxides to oxidation times between about 0.1 hour and 1.0 hours [7]. Film thickness was measured to an accuracy of better than 2% using a precision manual ellipsometer with a He-Ne laser (632.8 nm) source [1]. The samples used for the stress measurements were then masked, and the oxide was stripped from one side in order to induce curvature from the stress in the SiO₂ film [9]. The ir measurements were made on wafers in which the thermal oxide was present on both faces [4].

B. Stress Measurements

A two parallel laser beam reflection technique was used to determine the total stress in the oxide layer as a function of oxide film thickness; details of this method have been discussed in a paper by Kobeda and Irene [9]. The technique involves a measurement of the radius of curvature, R , of the Si substrate that has induced the stress in the SiO₂ layer. This curvature is induced by simply removing the oxide from one side of the oxidized silicon strip. The radius of curvature is then obtained from measurements of the separation between the two initially parallel laser beams reflected from the oxidized surface of the Si sample. Calibration is achieved by comparisons with flat mirror surfaces, and with mirrors of known curvature, $R = 20$ m and 50 m. These two mirror radii are within the range of curvatures present in most of the stressed Si/SiO₂ heterostructures. The total stress, σ_f , in the SiO₂ film is determined from a standard beam bending relationship [9,10]:

$$\sigma_f = (E' t_s^2)/(6(1-\gamma')t_f R); \quad (1)$$

where t_s and t_f are the substrate and film thicknesses, respectively and E' and γ' are Young's modulus and Poisson's ratio for Si, respectively. Since the thermal expansion coefficients of Si and SiO₂ differ significantly [9], there is an appreciable contribution to σ_f from thermal effects, i.e., stress that is induced by virtue of film growth at the elevated temperatures, 700°C and 1000°C, and stress measurements made at room temperature, approximately 20°C. The total film stress is $\sigma_f = \sigma_{th} + \sigma_i$, where σ_{th} is a thermally induced stress that can be calculated from the known values of the thermal expansion coefficients of Si and SiO₂, and σ_i the intrinsic growth stress, i.e., the stress that is generated through the

film growth process. This intrinsic growth stress is the focal point of this study.

We have been able to extend stress measurements to oxide thicknesses in the range of 100Å by the use of very thin 75 μm Si substrates. Since Eqn. (1) includes scaling factors of t_s^2 and $1/R$, a thinner substrate will yield a smaller radius of curvature, i.e., more curvature for a given stress level and film thickness. The reported values of stress in this paper are generally the average of four measurements made on each of three different samples. This multiplicity of stress measurements has enabled us to determine σ_i to an average uncertainty of about 0.5×10^9 dynes/cm².

C. Infrared Spectroscopy Measurements

The ir absorbance measurements reported here were obtained as described in Refs. 1-5. The measurements on the very thin oxides involve averages over several different samples. We have found that in some instances, noise reduction in the data through multiple point smoothing can lead to distortions of the spectra that become evident in samples such as these which have asymmetric absorption features. All of the data in this paper, except for the 60Å samples, rely on noise reduction through long term data acquisition rather than any form of post acquisition processing. We have taken care to eliminate distortion in the 60Å samples by the judicious choice and application of smoothing routines. Figure 1 indicates the ir absorbance for the bond-stretching vibration at about 1075cm^{-1} for a thermally grown SiO_2 thin film. There are two other first-order ir active vibrations in SiO_2 , a bond-bending band at about 800cm^{-1} , and a bond-rocking band at about 460cm^{-1} [1]. We have previously reported systematic changes in the 1075cm^{-1} band with different growth and annealing temperatures [1-5]. Changes in the character of other two bands are significantly smaller and therefore more difficult to use to monitor the effects of different growth and/or annealing temperatures. The insert in the figure shows the relative motion of the oxygen atom for the bond-stretching vibration; this motion is in the plane of the Si-O-Si bond, and in a direction parallel to a line joining the two silicon atoms.

In this report, we restrict our observations and the discussions following to the center frequency, ν , and the full-width at half-maximum (FWHM), $\Delta\nu$, of the bond-stretching feature; these are also indicated in Fig. 1. The values for ν and $\Delta\nu$, reported in the remainder of this paper, represent an average over six spectra taken on samples from the same furnace run. The experimental uncertainties in ν and $\Delta\nu$ come primarily from two sources, the signal to noise ratio in the data acquisition process, and the inherent resolution of the ir spectrophotometer for the particular set of conditions under which the data was taken. The signal to noise ratio is the dominant factor in the new data that we are reporting for the thin thermally grown oxides, and also varies with film thickness. For the thinnest films, 60Å, the uncertainties are approximately 1 cm^{-1} for both ν and $\Delta\nu$, where as for thicker films, greater than about 500Å, the respective uncertainties are 0.6cm^{-1} for ν , and 0.2cm^{-1} for $\Delta\nu$ [4].

III EXPERIMENTAL RESULTS

We have obtained new data for ν , $\Delta\nu$ and σ_i for thin oxide films grown at either 700°C or 1000°C. In Figs. 2-6, we have combined these new data with data previously reported [2-5] for thicker thermally grown SiO₂ films in order to emphasize the new features that emerge as we probe the oxide properties closer to the Si/SiO₂ growth interface.

Figures 2-6 then present the results of ir (ν and $\Delta\nu$) and stress (σ_i) measurements for films with thicknesses between about 60Å and 1300Å. The data shown in Figs. 2a and b were taken on thick oxides (approximately 1300Å thick) and indicate the way that ν and $\Delta\nu$ vary with the growth temperature, T_{OX} . Specifically, ν increases as T_{OX} is increased, and $\Delta\nu$ decreases as T_{OX} is increased. The results shown in Fig. 3 for $\Delta\nu$ as a function of ν were also taken on relatively thick oxides, average thickness 1300Å, and indicate a correlation between $\Delta\nu$ and ν that is obeyed universally by all of these thick oxides that we have studied [2-5]. These thin film layers include: (1) thermal oxides grown in dry and steam ambients at temperatures between 800°C and 1150°C; (2) thermal oxides that have been subsequently annealed at temperatures up to 1200°C; (3) oxides deposited by remote plasma-enhanced chemical-vapor deposition (RPECVD) between 100°C and 550°C; (4) and oxides deposited

by RPECVD and then annealed at temperatures up to 1000°C. The solid line is a linear regression analysis and is shown to quantify the correlated behavior of Δv and ν for these thick oxides.

Figure 4 presents the variation of the center frequency, ν , of the Si-O bond-stretching vibration as a function of film thickness for oxides grown at 700°C and 1000°C. The samples grown at 1000°C have larger values of ν at any given film thickness than the samples grown at 700°C. In all cases, however, as the film thickness is decreased, ν also decreases. Moreover, as the film thickness goes to zero both sets of data extrapolate to approximately the same frequency for the bond-stretching vibration, $1055\text{cm}^{-1} \pm 1\text{cm}^{-1}$. The solid lines in the figure are derived from a logarithmic regression analysis. Figure 5 displays the corresponding behavior for the variation of Δv as a function of film thickness for oxides grown at 700°C and 1000°C. For the oxides grown at 700°C, the value of Δv is relatively constant at about 79cm^{-1} , while for the oxides grown at 1000°C, Δv decreases significantly in the thinnest oxides. The data of Fig. 5 then demonstrate a break-down in the universal relationship between ν and Δv in the thinnest oxide films that we have studied.

Figure 6 includes a plot of intrinsic growth stress versus film thickness for oxides grown in a dry ambient at 700°C and 1000°C and for film thicknesses to approximately 100\AA [6]. At any given film thickness, the oxides grown at 700°C have a higher intrinsic growth stress than those grown at 1000°C, with the stress level in both sets of oxides increasing as the oxide thickness is decreased. The data at each growth temperature converge to the same value of the intrinsic stress, approximately $4.6 \times 10^9\text{ dynes/cm}^2$, as the oxide thickness goes to zero. This occurrence of a common maximum value of intrinsic growth stress at the Si/SiO₂ interface is not surprising since the origin of this interfacial stress is the constant molar volume change strain that occurs at the Si surface during the oxidation process [6]. It should also be noted from Fig. 4, that in addition to the extrapolated values of σ_i being the same for films grown at 700°C and 1000°C, the extrapolated values of ν are also the same. We will consider the implications of this in our discussion of the experimental data that follows.

IV DISCUSSION

We now proceed to discuss the data presented above in the context of a model for the thermal oxidation of silicon that emphasizes an aspect of that growth process that we characterize as a non-homogeneous thermal history. The model is based on a comparison between two time scales: (1) the time required to grow an oxide film of a specified thickness; and (2) the viscoelastic relaxation time at that same growth temperature. The notion of viscoelastic relaxation arises from the fact that there is a considerable increase in molar volume between the underlying silicon material and the growing oxide [6]; this in turn is responsible for the build up of a compressive stress in the oxide film in the immediate vicinity of the Si/SiO₂ interface. The stress at a given point in the oxide film can be relieved during the remainder of the oxide growth process only if the time for viscoelastic relaxation at the growth temperature is much shorter than the time required for completion of the oxidation process. There are two limiting cases that we wish to compare in a qualitative manner.

The first case is concerned with oxide growth at a relatively low temperature at which the viscoelastic relaxation time is longer than the oxidation time. Under these conditions, there is very little viscoelastic relaxation and any stress generated at the growth surface is not relaxed effectively during the subsequent film growth. Under these conditions there will be a relatively small stress gradient between the growth interface and the surface of the oxide film; i.e., between the "newest" and "oldest" regions of the oxide film. The other extreme is at a higher oxidation temperature where the time for viscoelastic relaxation can be comparable to, or even shorter than the oxidation time. Under these conditions the "new" oxide generated at the Si/SiO₂ interface is under stress due to the change in molar volume, but "older" oxide in the rest of the oxide layer can experience a substantial degree of stress relief via viscoelastic relaxation. We now demonstrate that the two cases discussed above are realized in oxides grown in dry oxygen ambients at temperatures of 700°C and 1000°C, respectively.

In order to study the distribution of intrinsic stress, and the associated strain in thermally grown oxide films, we determined the stress as a function of film thickness in oxides grown at different temperatures that span a significant range of growth rate and viscoelastic relaxation rate time scales. In addition, we have also studied the center frequency, ν , and FWHM, $\Delta\nu$, of the Si-O bond-stretching mode and have established in previous publications that the center frequency of this mode gives direct information about the bond-angle, 2θ , at the oxygen atom sites [1-5], and that relief of intrinsic stress is accompanied by systematic increases in ν , and therefore in 2θ , and also by decreases in $\Delta\nu$ [1-5].

The systematic variations in the stretching frequency, ν , and the intrinsic growth stress, σ_i , shown respectively in Figs. 4 and 6 for the films grown at 1000°C, demonstrate a continuous variation in the thermal history from highly stressed oxide at the growth interface, as displayed in the thinnest films, to a more relaxed and essentially annealed oxide characteristic of the bulk, as displayed in the thicker films. Since the stress in the SiO₂ film near the growth interface is in the primarily in the the the plane defined by that interface and defined here as the x-y plane, the effective stress in the z-direction, or the direction of film growth, must be *relatively* tensile. This follows from the tendency of a material to retain a constant volume, and is the concept upon which Poisson's ratio is defined. According to the simple Maxwell model of a solid [6], we expect stress relaxation to occur by viscous motion of the SiO₂ material away from the growth interface. The out-of-plane strain relaxation rate, $d\epsilon/dt$, in the Maxwell model is then proportional to the in-plane stress:

$$d\epsilon/dt = \sigma_i/\eta; \quad (2)$$

where η is the oxide viscosity. The smaller the value of the viscosity the higher the strain relaxation rate, and consequently the more rapid the relaxation of the intrinsic growth stress in the region removed from the Si/SiO₂ interface. The equilibrium viscosity is an exponential function of temperature, T , as shown in the following equation [8]:

$$\eta = \eta_0 \exp(E_\eta/R_g T); \quad (3)$$

where η_0 is a constant representing the minimum viscosity, E_η is an empirically determined activation energy and R_g is the gas constant. If the rate of stress relief is assumed to be proportional to the stress, as is usually the case, then;

$$d\sigma_i/dt = - (1/\tau) \sigma_i; \quad (4)$$

where τ is a constant, namely the viscoelastic relaxation time. This relaxation time is assumed to be independent of the time scale of the experiment. One can then integrate Eqn. (4) and obtain the following expression for the stress relief process;

$$\sigma_i(t) = \sigma_i(0) \exp (- t/\tau); \quad (5)$$

where $\sigma_i(0)$ is the maximum intrinsic stress at the growth interface, and t is the oxidation or annealing time. From the experimental data displayed in Fig. 6, we find an empirically determined value for $\sigma_i(0)$ of approximately 4.6×10^9 dynes/cm². Relaxation times have been predicted from viscosity measurements by assuming that the relaxation time, τ , is proportional to the viscosity [6];

$$\tau = \eta/G, \quad (6)$$

where G is the shear modulus. The shear modulus is a weak function of temperature, except for the significant decrease in value near 950-1000°C [11], so that the very strong exponential temperature dependence of η dominates over most of the temperature range [6]. In order to estimate relaxation times from the data displayed in Fig. 6, it is necessary to take into account that the measured values of stress represent an average integrated over the entire film thickness. Therefore, in order to be consistent with this aspect of the experimental data, the value of t used in Eqn. (5) and obtained from experimental data, must be an average oxidation time integrated over the film thickness. Such an average value for t can be obtained by integrating an empirical relationship for thickness as a function of oxidation time, e.g., the Grove-Deal model [12], and normalizing this integral through division by the total film thickness. Relaxation times estimated from this procedure appear in Table I. It is also possible to estimate relaxation times from the ir data, where we

have already shown that the center frequency of the bond-stretching vibration provides a measure of the bond-angle at the oxygen atoms sites. We develop this argument below, and indicate the validity of an assumption that is based on stress relaxation through changes in that bond-angle [5].

The systematic relationships between ν and $\Delta\nu$ displayed in Figs. 2 and 3 have been explained in previous publications in terms of a model based on the local atomic structure, in particular the bond-angle, 2θ , at the bridging oxygen atom sites (see Fig. 1) [1,2]. Within the framework of this model, the average or central frequency of the ir active bond-stretching vibration is given by:

$$\nu = \nu_0 \sin \theta, \text{ where } \nu_0 = 1116.5 \text{ cm}^{-1}; \text{ for } \theta = 75 \text{ degrees} \quad (7)$$

This relationship between ν and θ is based on a central force model for the vibrational modes of SiO_2 [13]. The model equation neglects motion of the oxygen atoms, and considers only two-body central bond-stretching forces, neglecting specifically the smaller three body bond-bending forces, etc. The neglect of these terms renormalizes the force field with the consequence of defining ν_0 empirically, rather than calculating it from microscopic forces, mode masses, etc. In any case the functional dependence of ν on θ is the important aspect of this model, and this is not compromised by the approximation inherent in Eqn. (7). The central force model also neglects small changes in the Si-O bond-length with changes in the bond-angle [14]. These changes in the bond-length are implicitly included in the empirical parameter, ν_0 . It should be noted that similar force constant approximations based on central forces alone, do not apply for the other two first order vibrational modes, so that any systematic changes in θ with growth and or annealing temperatures are not expected to have similar systematic effects on the frequencies of these other two first-order modes. This is consistent with our observation that changes in the bond-bending and rocking modes with growth and/or annealing conditions are smaller, and, as such it has not proven possible to use them as parameters for tracking relief of intrinsic growth stress. We use X-ray data, and assign the average Si-O-Si bond-angle a value of 150 degrees for an oxide grown at 1150°C. This choice of bond-angle is not critical in the

development that follows in the sense that it represents a bench mark position which simply serves as a point of reference for the comparisons that are made. The choice of 1150°C represents a temperature at which viscoelastic relaxation time is short compared to the time scale for growth. For a relatively thick oxide (1300Å) grown at 1150°C we find a vibrational frequency of 1078.5cm^{-1} . Combining this with a bond-angle of 150 degrees yields the value of ν_0 given in Eqn. (7).

At this point, we note that the average Si-Si (2nd neighbor) distance, $d_{\text{Si-Si}}$ is also a function of θ , through the relation:

$$d_{\text{Si-Si}} = 2 r_0 \sin\theta \quad (8)$$

where r_0 is the Si-O bond-length; r_0 has been shown to be a slowly varying function of θ [14], with the result that the assumption of a constant r_0 is consistent with the approximations used in Eqn. (7). The representation of the Si-Si distance through Eqn. (8) is important in our discussion of stress relief, since it has been shown that the density of SiO_2 thermally grown oxide films scales inversely with $[d_{\text{Si-Si}}]^3$ [1-5]. This has been established through correlated trends in the behavior of the index of refraction, n , of SiO_2 (in a transparent region of the spectrum, 632.8nm) with the vibrational frequency ν . Since ν is a function of θ through Eqn. (7), and since n is proportional to density [1], a correlation between ν and n is expected, i.e., n increases as ν decreases. Using Eqn. (7) and (8), we have been able to quantify that correlation by predicting the scale factor for the approximately linear relationship observed between ν and n [1]. The implication of a larger bond-stretching frequency is a larger average bond-angle at the oxygen atom sites, and hence a larger Si-Si distance and a reduced density. As will be discussed later, the changes in the Si-O-Si bond angle and density are themselves a manifestation of stress relief. We have developed an additional aspect of our model by interpreting the correlated data in Fig. 3 for bulk oxides and then, in Fig. 7, superimposing data from the thin oxides to highlight how the local atomic structures changes as the Si/SiO₂ interface is approached.

We have shown that the width of the Si-O stretching absorption band in the thick oxides could be understood in terms of a statistical distribution of Si-O-Si bond-angles. If $\Delta\nu$ comes from such a summation

over narrow vibrational bands, each associated with a different Si-O-Si bond angle, then $\Delta v = dv$ and we can simply differentiate Eqn. (7) to obtain the functional relationship between Δv and θ :

$$dv = v_0 \cos\theta d\theta. \quad (9)$$

Dividing Eqn. (9) by Eqn. (7), and then dividing and multiplying the right-hand side of that relationship by θ yields the following:

$$dv/v = \theta \cot\theta (d\theta/\theta) \quad (10)$$

We have replotted the data of Fig. 7 in Fig. 8 using the representation of Eqn. (10). The slope derived from this replotting of the Fig. 3 data is $d\theta/\theta = 0.22$; this value of the average bond-angle spread is in excellent agreement with X-ray data [15]. We have also included data from the thinnest oxides, where we find that the slope, $d\theta/\theta$, increases as the oxide thickness is reduced. This will be discussed in more detail later on in the paper. We first, however, return to the data in Fig. 4 where we have displayed v as a function of film thickness for oxides grown at 700°C and 1000°C.

In the context of the central force model for v , decreases in v with decreasing film thickness also reflect decreases in θ . From Eqn. (8) decreases in θ also imply a decreasing Si-Si distance and hence a more dense or more compacted film. This is consistent with the data that is displayed in Fig. 6 which shows increases in intrinsic compressive stress as the film thickness is reduced. The data in Fig. 6 are particularly interesting with regard to the extrapolated values of stress for zero film thickness. The observation that the data for oxides grown at both 700°C and 1000°C extrapolate to essentially the same value, then leads us to propose that the constant value of stress is primarily a manifestation of the increase in molar volume that occurs in the conversion of Si to SiO₂ [6].

The data in Fig. 5 indicates that Δv remains relatively constant as a function of film thickness for the oxides grown at 700°C, but that Δv decreases dramatically for the very thinnest oxides grown at 1000°C. These observations, coupled with the data displayed in Fig. 4 indicate that

as oxide thickness is reduced the linear relationship between $\Delta\nu$ and ν , displayed in Figs. 3 for thick oxides, starts to break down. This is evident from the data displayed in Fig. 7, where we have plotted $\Delta\nu$ versus ν for the thin oxides. We have also included in Fig. 7 the result of a linear regression analysis of the thick oxide data of Fig. 3. The data for the thin oxides fall below the average behavior of the thick oxides indicating that the center frequency of the absorption band has shifted to lower wavenumbers relative to the distribution of bond-angles. If the data from the thin oxides had the same slope as the regression analysis line but was displaced by a constant amount, then we would expect smaller values of ν to have correspondingly smaller values of $\Delta\nu$. But, since the relative distribution of bond-angles, $\Delta\theta/\theta$, depends both on the spread in bond-angles, $\Delta\theta$, and the value of θ itself [see Eqn. (10)], a slightly smaller value of $\Delta\nu$ does not necessary imply a smaller relative distribution of bonds angles. In fact we shall demonstrate just the opposite exists. But before proceeding, it should be noted that Boyd [16] has also reported similar trends in the ir absorption spectra of thin oxides, but his observations were based on direct transmission data, rather than calculated values of the absorbance, and, as such any quantitative comparisons with the trends he has reported are not possible. Another way of looking at the behavior displayed in Fig. 8 is based on the changes in the local atomic structure, specifically the Si-O-Si bond angle 2θ , as the growth interface is approached. This can be treated in a quantitative manner by including the thin oxide data in a plot of $d\nu/\nu$ versus $\theta \cot\theta$, and then using the slope of that plot as a basis for determining a value for $d\theta/\theta$. This is shown in Fig. 8, where we have included the regression analysis fit to the thick oxide data as a reference, and then displayed representative thin oxide data. We find a value of $d\theta/\theta = 0.47$ for the thinnest oxides. This is significantly greater than the value of $d\theta/\theta = 0.22$ for the thick oxides, and in fact is too large to have any direct physical significance; i.e., the model used to analyze the data no longer applies. Specifically, we interpret this large value of $d\theta/\theta$ to mean that the distribution of bond-angles near the Si/SiO₂ interface is no longer statistical in nature, and is determined instead by other types of bonding constraints associated with the differences in molar volume between crystalline silicon and SiO₂, and therefore indicates that the spread in the

bond-angle at the oxygen atom sites is being increased by the build-up of growth stress as the Si/SiO₂ interface is approached. At first glance a seemingly greater relative spread in bond-angles appears to be counter-intuitive, since one would have expected constraints in the local atomic structure, developed from the compressive stress at the growth interface, to always decrease the spread in Si-O-Si bond angles. This point clearly needs additional study, both experimentally and through modelling of the way the intrinsic stress, generated by the strain at the growth interface, is relieved during subsequent growth and annealing.

The ir data obtained for the bond-stretching vibrations and displayed in Fig. 4 can also be analyzed in terms of a Maxwell model for viscoelastic relaxation. We assume a relationship of the form:

$$v_{\max} - v = (v_{\max} - v_{\min}) \exp(-t/\tau) \quad (11)$$

where v_{\max} is determined from the high temperature (1150°C) thick (1300Å) oxide data and is set equal to 1079cm⁻¹, the approximate asymptote in the v versus growth temperature plot [see Fig. 2]; v_{\min} is estimated from the thinnest oxides (60Å) grown at 700°C, and has a value of approximately 1055cm⁻¹. As in Eqn. (5), t is an average growth (or annealing) time and τ is a viscoelastic relaxation time. We have calculated values of τ from the ir data and these are displayed in Table I along with those obtained from the stress data. The relaxation times computed for a growth temperature of 1000°C, based on the data from a 607Å oxide film are in very close agreement with an average value for τ of approximately 0.75 hours or equivalently, approximately 2.7×10^3 s. The data for 700°C growth, based on comparison with an oxide film that is 701Å show a somewhat greater spread (about $\pm 50\%$) with an average value of about 800 hours or approximately 2.9×10^6 s. Values of τ estimated from viscosity and shear modulus data [6] are also displayed in Table I. There is order of magnitude agreement between the two methods of estimating τ at 1000°C, 0.2 hours from the viscosity/shear modulus approach as compared to 0.65 hours from Eqn. (11). However, the viscosity data yields a significantly higher value of τ at 700°C, approximately 1270 hours as compared to 332 hours from Eqn. (11) [6]. We suspect the differences between these determinations for τ at 700°C arise at least in part from

possible errors in the extrapolation of viscosity and shear modulus data. We now compare the relative time scales for relaxation and growth, and discuss our observations relative to the different stress gradients in the films grown at 700°C and 1000°C in terms of these two time scales.

We note the times required to grow thermal oxides in a dry oxygen ambient at 1000°C range between 0.25 and 2.0 hours for oxide thickness between 200Å and 1000Å, whilst times between 100 and 500 hours are required for the same thickness range at 700°C. For example, the growth time was approximately 1.2 hour for a 700Å oxide grown at 1000°C, whereas for a 600Å oxide grown at 700°C, the time was approximately 350 hours. This means that the time scale for the growth of the oxide at 1000°C would allow relaxation of the "old oxide" in thicker films, but not the "newer oxide" near the growth interface [the viscoelastic relaxation time at 1000°C is approximately 0.75 hours]. In contrast in the films grown at 700°C, the growth time scale is too short for appreciable relaxation [the average viscoelastic relaxation time at 700°C is about 800 hours]. These differences in the relative growth and relaxation times are clearly visible in the data displayed in Figs. 4 and 6. Implicit in the estimates of τ that we have made from the stress and ir data is an assumption that the ir data reflects in some way the strain that is associated with the growth induced intrinsic stress. This assumption is supported through an analysis that is given below.

One way to demonstrate that the ir data and stress data are complementary in giving information about stress and stress relief is to demonstrate that the ir data and stress data can be combined to yield one of the elastic constants of SiO₂. We have previously demonstrated a proportionality between the average intrinsic stress in thick oxide films and the strain as estimated from the ir data [4]. We now present the assumptions used in that analysis and extend it to include the new thin oxide data. Using the model described in Eqns. (7) and (8), we proceed in the following manner. We first assume that changes in the Si-Si distance are an appropriate relative strain parameter and that these may be deduced from the ir data via the dependence of both ν and d_{Si-Si} on θ . We therefore define the relative strain, ϵ , as given by:

$$\epsilon = \Delta d_{\text{Si-Si}} / d_{\text{Si-Si}} \quad (12)$$

We define $2\theta_1$ as the Si-O-Si bond-angle in an oxide grown at 1150°C, and r_0 as the corresponding Si-O bond-length. If we neglect any changes in the Si-O bond-length with changes in the Si-O-Si bond angle, then if $2\theta_2$ as the Si-O-Si bond-angle in an oxide grown at a lower temperature; e.g., 700°C. Substitution of Eqn. (8) into Eqn. (12) yields the following approximate value for the strain:

$$\epsilon = (2r_0 \sin\theta_1 - 2r_0 \sin\theta_2) / 2r_0 \sin\theta_1 \quad (13)$$

We have previously shown that it was valid to neglect any changes in the Si-O bond-length when considering the applicability of the central force model for relating the Si-O bond-stretching frequency to the Si-O-Si bond-angle. However, for the purposes of estimating the strain, these small changes in the Si-O distance must be taken into account. Consider first the approximation given by Eqn. (13), where the changes in the Si-O bond-length are neglected. Since $\nu_m = \nu_0 \sin\theta_m$, for $m = 1, 2$, we substitute values of $\sin\theta_m$ directly into Eqn. (13) and obtain the following approximate relationship between the strain, ϵ , and the vibrational frequencies ν_1 and ν_2 , namely:

$$\epsilon = (\nu_1 - \nu_2) / \nu_1 \quad (14)$$

We note that compressive in-plane stress is usually accompanied by tensile relaxation in the out-of-plane direction. This renders an optically isotropic material uniaxial. In the geometry we are using for the ir studies, the electric field vector is always in-plane, and that the ir absorption spectrum derives from modes with in-plane polarizations. As such the properties of these modes reflect the in-plane stress, and as shown in Eqn. (14) also yield information relative to the in-plane strain. Since the relationship in Eqn. (14) treats differences in the frequencies, it is important to determine the magnitude of the terms neglected by not treating explicitly any of the changes in the Si-O bond-length [14]. These changes come from differences in the hybridization of the oxygen atom 2s and 2p wavefunctions as 2θ is changed. As 2θ increases, the amount of 2s character increases, and this in turn means that the Si-O bond-length increases as the Si-O-Si bond-angle is decreased [14]. Therefore Eqn. (14)

always overestimates the strain. We now demonstrate this in Eqn. (15), and also through that same relationship provide a quantitative way to determine the strain to the next level of approximation. If we consider the change in the Si-O bond-length explicitly, then we may rewrite Eqn. (13) as:

$$\epsilon = (2r_0 \sin\theta_1 - 2[r_0 + \delta r] \sin \theta_2)/2r_0 \sin \theta_1, \quad (15)$$

where δr is the change in the Si-O bond-length associated with the change in the Si-O-Si bond-angle, $\delta\theta = \theta_1 - \theta_2$. We can then rewrite Eqn. (15) in terms of vibrational frequencies and obtain,

$$\epsilon = (v_1 - v_2)/v_1 - (\delta r/r_0)(v_2/v_1). \quad (16)$$

Combining terms defining $\delta r = (\Delta r/\Delta\theta) \delta\theta$, we have,

$$\epsilon = 1 - (1 + [(\Delta r/\Delta\theta) \delta\theta/r_0])(v_2/v_1). \quad (17)$$

The relationship in Eqn. (17) enables us to estimate the strain from the ir measurements, provided that we take into account the correction term, $[(\Delta r/\Delta\theta) \delta\theta/r_0](v_2/v_1)$, which we can obtain from the results presented in Ref. 14. We determine the value of v_2 from ir absorption data and then determine the relative strain for any growth temperature and oxide thickness relative to the reference frequency v_1 , which is taken to be the average ir frequency for a thick oxide grown at 1150°C. The bulk material for a thick oxide grown at this temperature has a thermal history such that the growth time is long compared to the viscoelastic relaxation time, and the region in which there is a stress gradient is then small with respect to the total oxide thickness. This is displayed in Fig. 4 where this behavior is clearly evident in the comparison between thermal oxides grown at 700°C and 1000°C. Note again the growth time for the oxide formed at 700°C is short relative to τ , so that there has been no stress relaxation in that oxide film during its growth period.

We now are in a position to compare stress and strain in the SiO₂ films, and thereby deduce an elastic constant from the stress and ir data. The computation of a *renormalized* Young's modulus, $E/(1-\gamma)$ [6], for SiO₂ then provides a check for the validity of our approach regarding the way that changes in the ir frequency give information relative to strain within

the oxide film; γ is Poisson's ratio for SiO_2 , 0.18 [17,18]. We will estimate $E/(1-\gamma)$ from the data for the oxide film grown at 1150°C . The relationship between Young's modulus, Poisson's ratio, the film stress and the relative strain is given by:

$$\sigma_f = \varepsilon E/(1-\gamma) \quad (18)$$

where σ_f is determined from Eqn. (1) and ε , the relative stress, is given by Eqn. (17). σ_i , the intrinsic stress at the Si/SiO₂ interface is determined from the intercept in Fig. 6 and taken to be 4.6×10^9 dynes/cm². The film stress, σ_f is obtained by combining σ_i with the thermally generated stress of approximately 4×10^9 dynes/cm². We use Eqn. (17) to determine the relative strain. We take θ_1 to be equal to 150 degrees, corresponding to a value of $\nu_1 = 1078.5$ cm⁻¹ (see Eqn. (7), and $\theta_2 = 141.7$ degrees, corresponding to $\nu_2 = 1055$ cm⁻¹, the value of ν , extrapolated from the data of Fig. 4. From the data of Ref. 14, we estimate $[(\Delta r/\Delta\theta)/r_0] = 7.76 \times 10^{-4}$ degrees⁻¹, and from the values of θ_1 and θ_2 from the ir data, we set $\delta\theta = 8.3$ degrees. Proceeding in this way we obtain a value for $E/(1-\gamma)$ of approximately $(5.5 \pm 0.5) \times 10^{11}$ dyne/cm², which is good agreement with the quoted value of approximately 8.5×10^{11} dyne/cm² [17,18]. This comparison demonstrates the self-consistency of our model, and the use of the Si-Si distance as a measure of the relative strain.

The approach used in the determining a value for $E/(1-\gamma)$ for SiO₂ from the total stress data and the relative strain, as calculated from Eqn. (17), is valid for the film grown at 1000°C , because there is clearly viscoelastic relaxation of the interfacial stress in the growth direction and one can then expect linear elastic theory to apply. This in turn justifies the use of the renormalized Young's modulus as given in Eqn. (18) [6]. On the other hand, the time scales for oxide film growth and viscoelastic relaxation for oxides grown at 700°C are such that viscoelastic relaxation in the growth direction does not occur during film growth. This in effect means that the 700°C data can not be treated in the same way using a renormalized Young's modulus which specifically takes into account relaxation in the z-direction. To illustrate this in a graphical way, we have taken intrinsic stress data from Fig. 6, and approximate strain data, estimated from Eqn. (14) and Fig. 4, and plotted these in Fig.

9. We have separately analyzed the data for the 1000°C and the 700°C oxides, and the results of these linear regression analyses are included in the diagram. As expected from our discussion above, we find that the slope of the 1000°C data is greater than that of the 700°C data. This is interpreted to represent the differences in the viscoelastic relaxation phenomena at the two growth temperatures; i.e., the slope of the 1000°C data is proportional to $E/(1-\gamma)$, and the stress extrapolates to zero for zero strain, whereas the slope of the 700°C data is greater, and the 700°C stress does not extrapolate to zero for zero strain. Correcting the 1000°C data for total stress, and taking into account the bond-length changes as well, brings the calculated slope into good agreement with the value for $E/(1-\gamma)$ as obtained above. On the other hand, the regression analysis fit to the 700°C data does not go through the origin indicating that the lack of viscoelastic relaxation in the z-direction and making it not possible to interpret this 700°C data by our method of analysis. The increased slope for the 700°C data is never the less consistent with a compressive in-plane stress and a lack of viscoelastic relaxation in the z-direction.

V SUMMARY

By way of summary, we make the following points:

(1) The compressive stress in thermally grown SiO_2 films is a result of the strain induced by the differences in the molar volumes of Si and SiO_2 at the grown interface. This leads to a value for the intrinsic growth stress at that growth interface that is independent of the growth temperature and the growth rate. Recent experiments, to be discussed in a later publication [20], indicate that this value of the stress at the Si/ SiO_2 interface is not changed during high temperature [1100°C] thermal annealing. This means that the effects of the molar volume mismatch at the Si/ SiO_2 interface are not changed via annealing even at temperatures where substantial viscoelastic relaxation can occur during the time period of the annealing cycle.

(2) The extent to which an oxide film displays a stress gradient depends on the relative time scales for oxide growth and viscoelastic relaxation. Specifically, for oxides grown at low temperatures, e.g., 700°C

to 850°C, the viscoelastic relaxation times are very long with respect to the growth times, and stress relief in the growth direction via a viscoelastic mechanism is not possible. These films in effect have a uniform thermal history. This is characterized experimentally by only small differences with film thickness in: (i) the intrinsic stress; and (ii) the *ir* frequency of the bond-stretching vibration which provides a measure of the relative strain. On the other hand, for oxides grown at, or above about 950°C to 1000°C, viscoelastic relaxation times are comparable or shorter than the growth times, and substantial viscoelastic relaxation occurs. This leads to stress gradients and the associated variation in the *ir* vibrational frequencies which reflect an accompanying variation in the strain. These high temperature films then display evidence for a non-uniform thermal history.

(3) The viscoelastic relaxation times estimated from stress data, and from *ir* data are approximately the same, and support the application of a Maxwell model for viscoelastic relaxation.

(4) The computation of viscoelastic relaxation times and an in-plane Young's modulus from stress and *ir* data further supports the use of the Si-Si distance, which is influenced mostly changes in the Si-O-Si bond-angle, as a relative strain parameter.

(5) The breakdown of a universal relationship between the full-width of the bond-stretching *ir* absorbance and the *ir* frequency in thin oxide films indicates a change in the distribution of bond-angles in the immediate vicinity of the Si/SiO₂ interface. The result described above is counter-intuitive with the *relative* distribution of angles increasing in the vicinity of the Si/SiO₂ interface where the stress and strain are pinned by differences between the two molar volumes at the growth interface.

(6) It is well-established that Si/SiO₂ interfaces formed at 1000°C and incorporated in metal-oxide-semiconductor (MOS) structures have relatively defect free interfaces with the densities of interfacial trapping sites as deduced from C-V measurements generally being much less than about $5 \times 10^{10}/\text{cm}^2$ [19]. On the other hand Si/SiO₂ interfaces formed at 700°C generally have trapping state densities that are more

than an order of magnitude higher. This means that the generation of the bonding defects that lead to trapping are not simply related to either the magnitude of the intrinsic growth induced stress at the Si/SiO₂ interface, or the stress gradient in the immediate vicinity of that interface. Unfortunately, our study does not supply any direct information relative to other possible interfacial defect generation mechanisms. However, our results suggest that the defect generation mechanism may in part related to the lack of stress relief in the low temperature thermal oxides, $t_{ox} < 900^{\circ}\text{C}$.

We are continuing this study, and have set up experimental studies to examine the effects of annealing on thermally grown oxides [20]. Our objective is to vary annealing times and temperatures for oxides grown at low temperature, and thereby to extend the observations made in this paper from thermal growth to thermal annealing as well. We are particularly interested in measuring the changes in the stress and strain profiles that result from high temperature thermal annealing, and in determining the extent to which the relative times scales for annealing and for viscoelastic relaxation, at the annealing temperatures, provide a quantitative basis for understanding the changes brought about by the annealing process.

ACKNOWLEDGEMENTS

This research has been supported in part under contracts from the Office of Naval Research; N00014-79-C-0133 and N00014-86-K-0760 at North Carolina State University, and N0014-83-C-0571 at the University of North Carolina at Chapel Hill. We acknowledge the use of facilities at the Microelectronics Center of North Carolina (MCNC). We also acknowledge helpful discussions with Professor R Fornes of the Department of Physics of NC State University.

REFERENCES

1. G. Lucovsky, M.J. Mantini, J.K. Srivastava and E.A. Irene, *J. Vac. Sci. Technol.* **B5**, 530 (1987).
2. J.T. Fitch and G. Lucovsky, *MRS Symp. Proc.* **92**, 89 (1987).
3. J.T. Fitch and G. Lucovsky, *MRS Symp. Proc.* **105**, 151 (1988).
4. J.T. Fitch and G. Lucovsky, *AIP Conf. Proc.* **167**, AVS Sub-Series, ed. by G.W. Rubloff (1988) (in press).
5. G. Lucovsky, J.T. Fitch, E. Kobeda and E.A. Irene, *J. Electrochem. Soc.*, (1988), in press.
6. E.A. Irene, E. Tierney and J. Angiello, *J. Electro. Chem. Soc.* **129**, 2594 (1982); E. Kobeda and E.A. Irene, *J. Vac. Sci. Technol.* **B6**, 574 (1988).
7. D.W. Hess and B.E. Deal, *J. Electrochem. Soc.* **124**, 735 (1977); B.E. Deal, *J. Electrochem. Soc.* **125**, 576 (1978).
8. W.D. Kingery, H.K. Bowen and D.R. Uhlman, *Introduction to Ceramics* (John Wiley and Sons, New York, 1976), p. 835.
9. E. Kobeda and E.A. Irene, *J. Vac. Sci. Technol.* **B4**, 720 (1986).
10. G.G. Stoney, *Proc. Roy. Soc. London*, **A82**, 172 (1909).
11. *Handbook of Glass Data, Part A*, ed. by O.V. Mazurin, M.V. Streltsina and T.P. Shvaiko-Shvaikovskaya (Elsevier, Amsterdam, 1983).
12. S.K. Ghandi, *VLSI Fabrication Principles* (John Wiley and Sons, New York, 1983), p. 380.

13. F.L. Galeener, Phys. Rev. **B19**, 4292 (1979); F.L. Galeener and P.B. Sen, Phys. Rev. **B17**, 1928 (1978).
14. M.D. Newton and G.V. Gibbs, Phys. Chem. Miner. **6**, 221 (1980).
15. R.L. Mozzi and B.E. Warren, J. Appl. Cryst. **2**, 164 (1969).
16. I.W. Boyd and J.I.B. Wilson, J. Appl. Phys. **62**, 3195 (1987).
17. S. Isomae, J. Appl. Phys. **57**, 216 (1985).
18. R.J. Jaccodine and W.A. Schlegel, J. Appl. Phys. **37**, 2429 (1966).
19. B.E. Deal, in *Semiconductor Materials and Process Technology Handbook for VLSI and ULSI*, ed. by G.E. McQuire (Noyes Publications, Park Ridge, 1988), p. 46.
20. J.T. Fitch and G. Lucovsky, Unpublished data.

FIGURE CAPTIONS

Fig. 1 IR absorbance for SiO_2 bond-stretching vibration. The figure includes the position of the spectral peak, ν , the full-width at half-maximum, $\Delta\nu$, and an insert that indicates the motion of the oxygen atom. 2θ is the bond-angle at the oxygen atom site.

Fig. 2a and 2b ν (2a) and $\Delta\nu$ (2b) versus oxidation temperature, respectively for dry oxides.

Fig. 3 $\Delta\nu$ versus ν for thermal and plasma oxides, including both types of oxides which have been annealed. The line is a regression analysis of the data.

Fig. 4 ν versus oxide thickness for thermal oxides grown in dry oxygen at 700°C and 1000°C . The solid lines represent logarithmic interpolations of the data. The approximate intercept for both sets of data is 1055 cm^{-1} .

Fig. 5 $\Delta\nu$ versus oxide thickness for thermal oxides grown in dry oxygen at 700°C and 1000°C .

Fig. 6 Intrinsic stress, σ_i , versus oxide thickness for thermal oxides grown in dry oxygen at 700°C and 1000°C . The extrapolated stress at the Si/SiO_2 interface is estimated to be about $4.6 \times 10^9 \text{ dynes/cm}^2$.

Fig. 7 $\Delta\nu$ versus ν . The solid line is the regression analysis from Fig. 3, and the points are for thin oxides grown in dry oxygen at 700°C and 1000°C . The arrows indicate the direction of increasing film thickness.

Fig. 8 $\Delta\nu/\nu$ versus $\theta \cot \theta$ [see Eqn. (10)]. The solid line is a regression analysis of data for thick oxides; this yields a slope, $\Delta\theta/\theta = 0.22$. The points are for thin oxides; display on the average an increased slope = 0.47.

Fig. 9 Intrinsic stress, σ_i , versus $(\nu_1 - \nu_2)/\nu_1$ as determined from the IR data [see Eqn. (14)]. We have separately analyzed the data for the 1000°C and 700°C oxides, and the lines derived from a linear regression analysis are shown. The slope for the 1000°C data is greater than that for the 700°C data. In order to obtain estimates of the elastic constants from these slopes, it is necessary to include: (a) the thermal contribution to the stress data; (b) the effects of viscoelastic relaxation in the z-direction;

and (c) the contributions of bond-length changes as a function bond-angle changes to the strain data.

Table I Estimated Viscoelastic Relaxation Times, τ

Oxidation Temperature	τ, Stress data This study	τ, IR data This study	τ, Viscosity data, Ref. 6
700°C	1,270 hours	332 hours	5,300 hours
1000°C	0.86 hours	0.65 hours	0.20 hours

Fig. 1

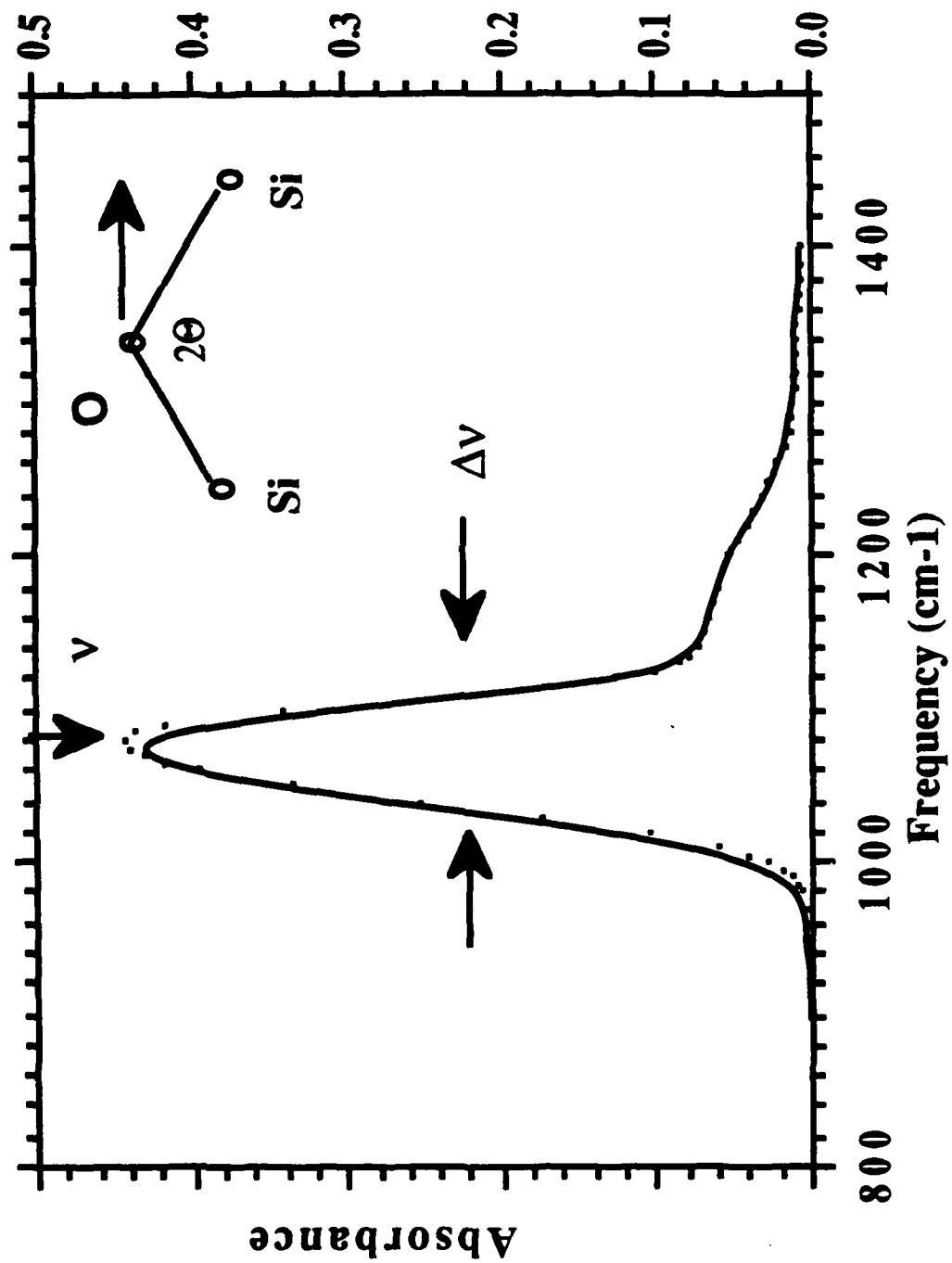


Fig. 2a

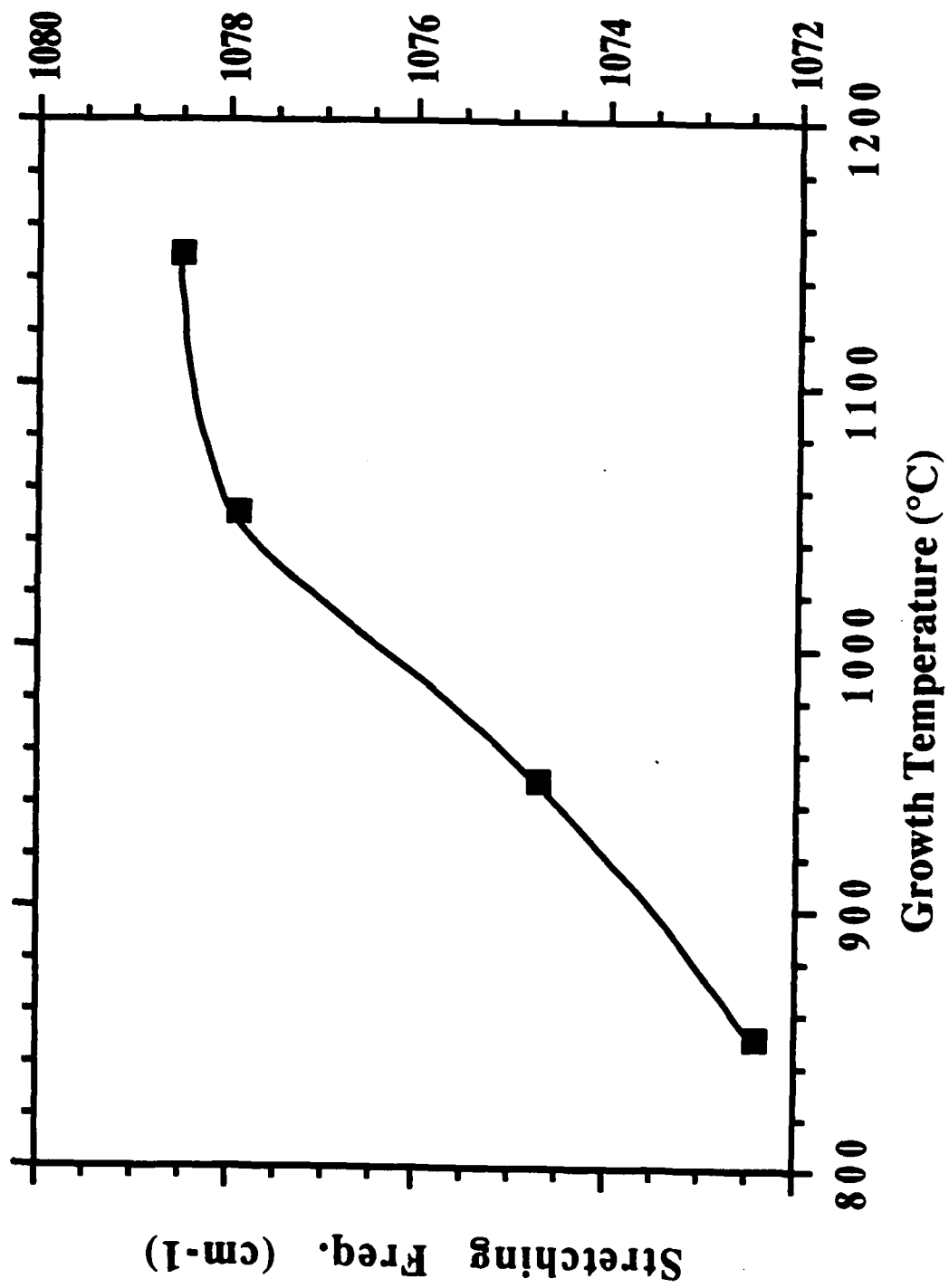


Fig. 2b

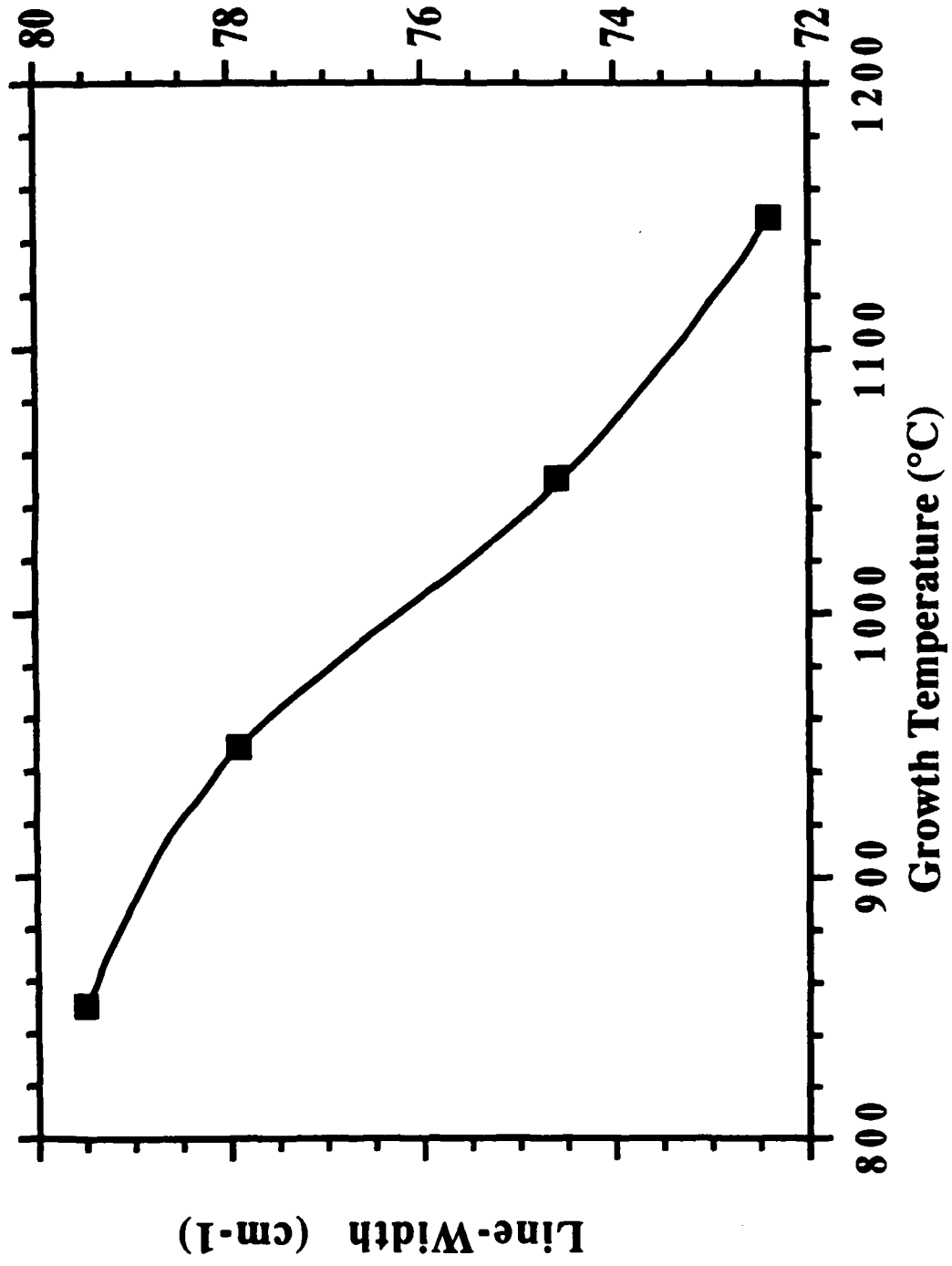


Fig. 3

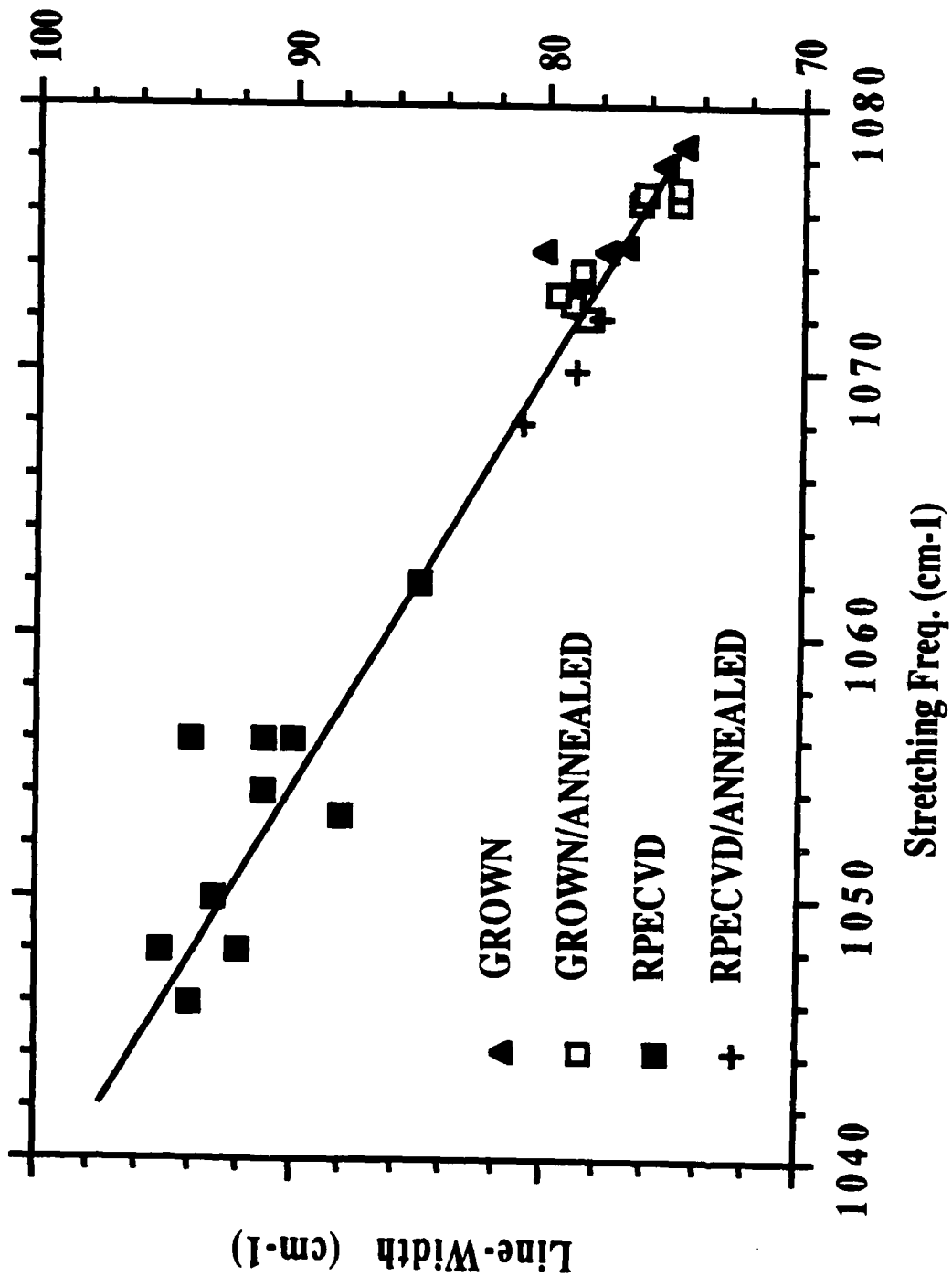


Fig. 4

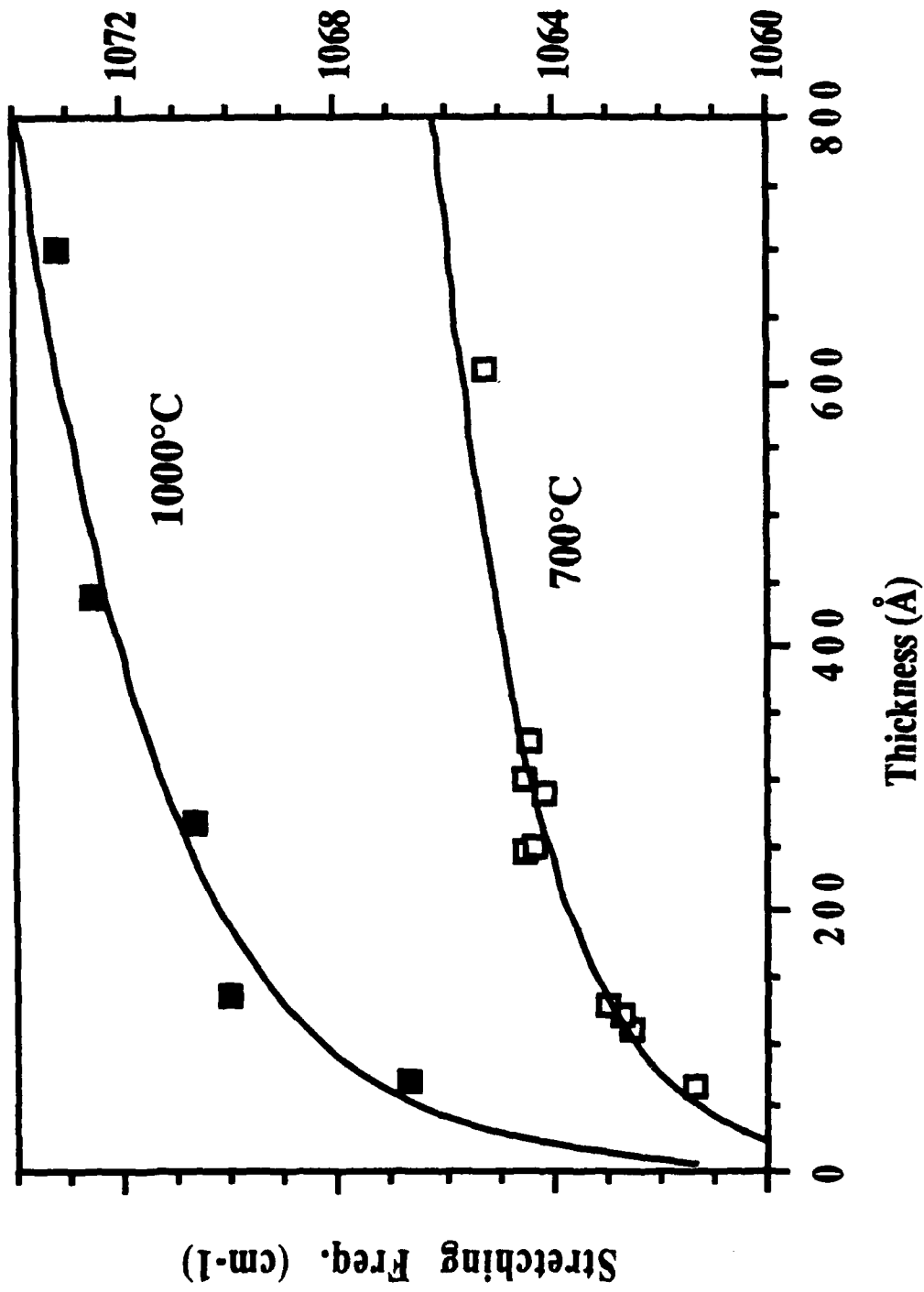


Fig. 5

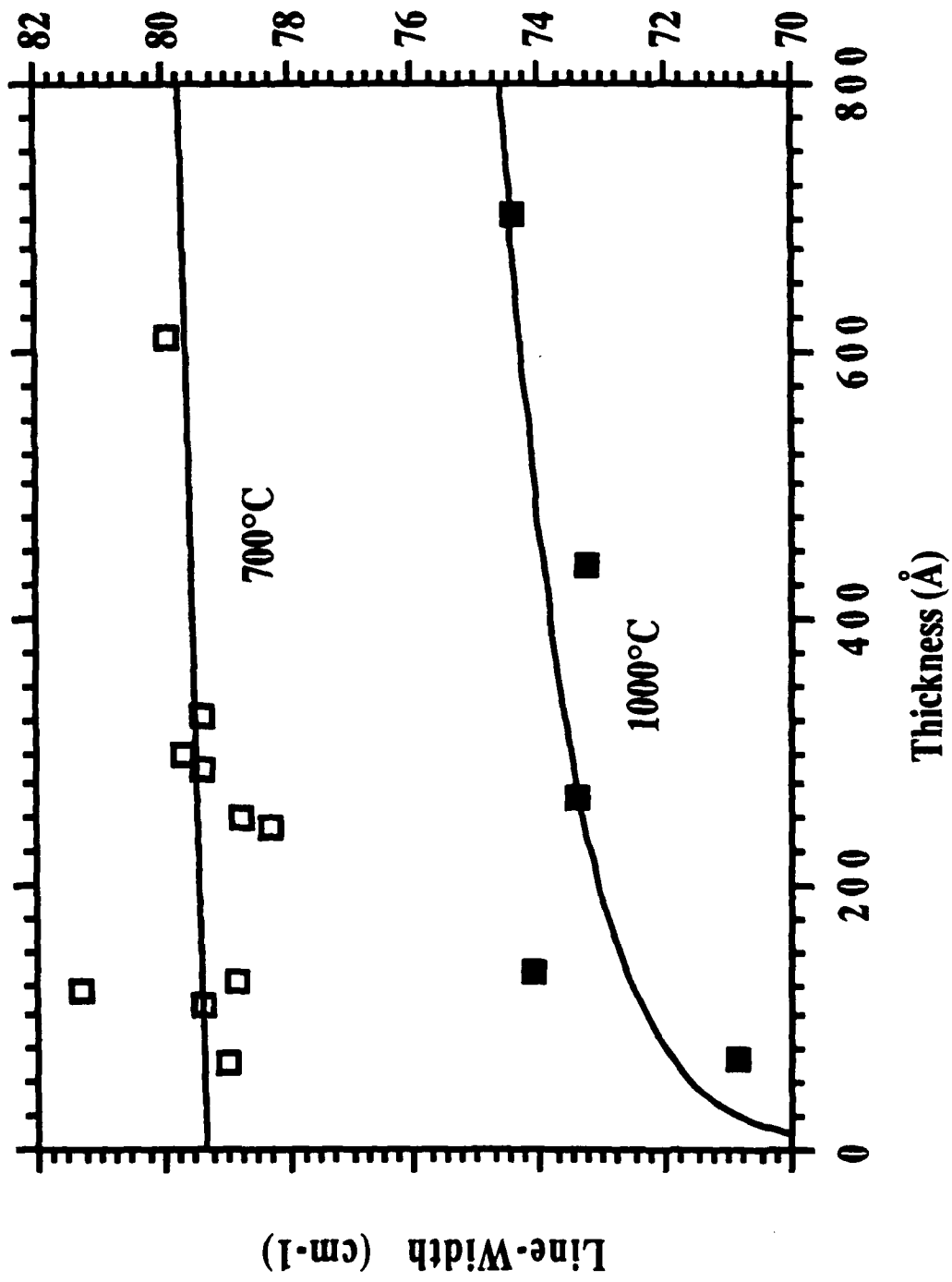


Fig. 6

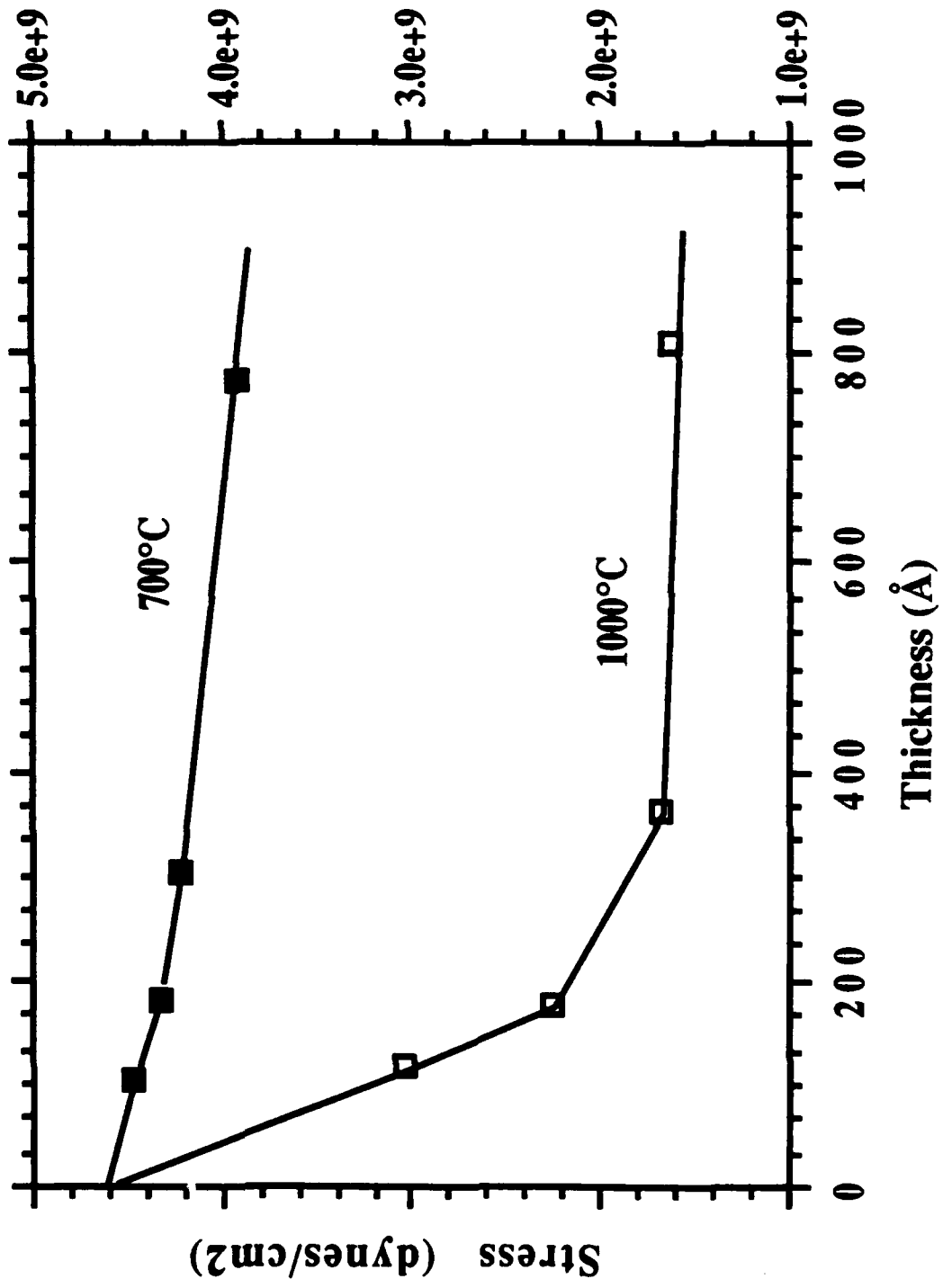


Fig. 7

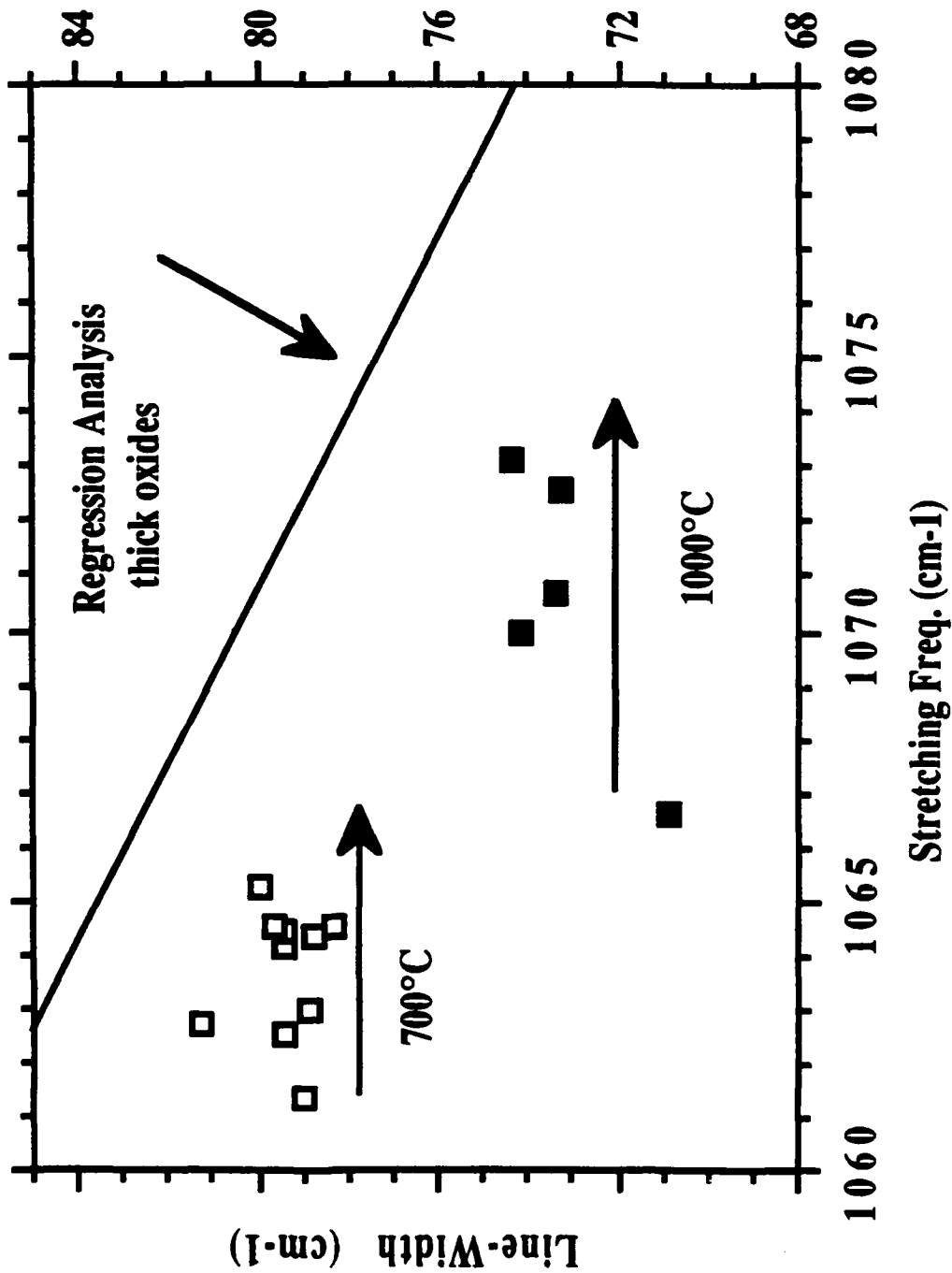


Fig. 8

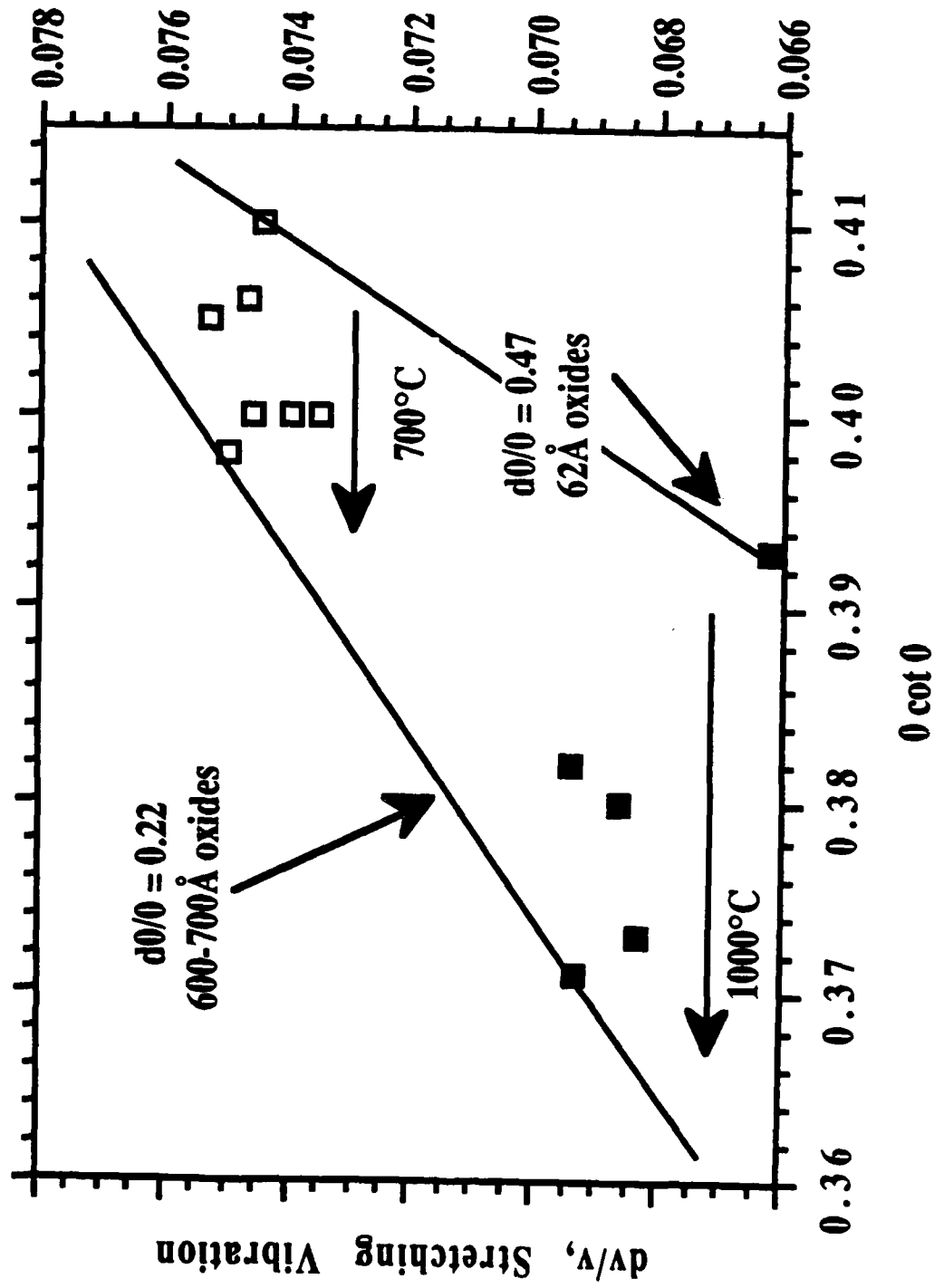


Fig. 9

